

Novel Superstructure-Phase Two-Dimensional Material 1T-VSe₂ at High Pressure

HPSTAR
1086-2020

Raimundas Sereika,^{*,†,‡,§,||} Changyong Park,^{§,||} Curtis Kenney-Benson,[§] Sateesh Bandaru,^{⊥,||} Niall J. English,^{||} Qiangwei Yin,[#] Hechang Lei,^{#,||} Ning Chen,[@] Cheng-Jun Sun,[∇] Steve M. Heald,^{∇,||} Jichang Ren,[●] Jun Chang,[○] Yang Ding,^{*,†} and Ho-kwang Mao^{†,■}

[†]Center for High Pressure Science and Technology Advanced Research, Beijing 100094, China

[‡]Vytautas Magnus University, K. Donelaičio Street 58, Kaunas 44248, Lithuania

[§]High Pressure Collaborative Access Team, X-ray Science Division, Argonne National Laboratory, Lemont, Illinois 60439, United States

^{||}School of Chemical and Bioprocess Engineering, University College Dublin, Belfield, Dublin 4, Ireland

[⊥]College of Materials and Environmental Engineering, Institute for Advanced Magnetic Materials, Hangzhou Dianzi University, Hangzhou 310018, China

[#]Department of Physics and Beijing Key Laboratory of Optoelectronic Functional Materials & Micro-nano Devices, Renmin University of China, Beijing 100872, China

[@]Canadian Light Source, 44 Innovation Boulevard, Saskatoon, SK S7N 2V3, Canada

[∇]X-ray Science Division, Advanced Photon Source, Argonne National Laboratory, Lemont, Illinois 60439, United States

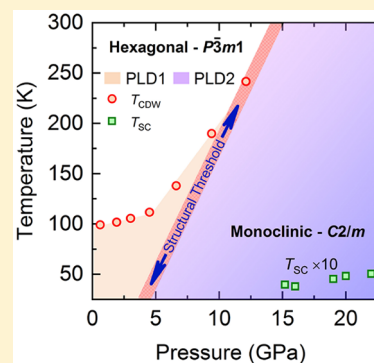
[●]Nano and Heterogeneous Materials Center, School of Materials Science and Engineering, Nanjing University of Science and Technology, Nanjing 210094, People's Republic of China

[○]College of Physics and Information Technology, Shaanxi Normal University, Xi'an 710119, P. R. China

[■]Geophysical Laboratory, Carnegie Institution of Washington, Washington, D.C. 20015, United States

Supporting Information

ABSTRACT: A superstructure can elicit versatile new properties in materials by breaking their original geometrical symmetries. It is an important topic in the layered graphene-like two-dimensional transition metal dichalcogenides, but its origin remains unclear. Using diamond-anvil cell techniques, synchrotron X-ray diffraction, X-ray absorption, and first-principles calculations, we show that the evolution from weak van der Waals bonding to Heisenberg covalent bonding between layers induces an isostructural transition in quasi-two-dimensional 1T-type VSe₂ at high pressure. Furthermore, our results show that high pressure induces a novel superstructure at 15.5 GPa rather than suppresses it as it would normally, which is unexpected. It is driven by Fermi-surface nesting, enhanced by pressure-induced distortion. The results suggest that the superstructure not only appears in the two-dimensional structure but also can emerge in the pressure-tuned three-dimensional structure with new symmetry and develop superconductivity.



Two-dimensional transition metal dichalcogenides (TMDs) exhibit rich physics, which provide an ideal “playground” for studying novel quantum states, and exhibit promising features for future advanced technological applications.^{1–3} Indeed, various modulation superstructures have been realized in TMDs.^{4,5} Periodic lattice distortion (PLD) is often accompanied by charge density waves (CDW), increasing the Coulombic and elastic energy as a consequence and being compensated by a decrease in the energy of occupied electronic states. According to Peierls instability, the distortion-induced kinetic energy gain is proportional to the non-interacting electronic susceptibility; Fermi-surface nesting would enhance the energy gain by sharply increasing the

electronic susceptibility. However, in the TMDs with a superlattice, density functional theory (DFT) calculations have suggested that singularities in the susceptibility are not such a prerequisite for realizing superstructures, while angle-resolved photoemission spectroscopy also found no sharp Fermi-surface nesting. Therefore, the origins of the TMD superstructures, which are commonly attributed to either electron–phonon coupling or Fermi-surface nesting, warrant further elucidation and clarification. Moreover, many studies

Received: November 3, 2019

Accepted: December 10, 2019

Published: December 10, 2019

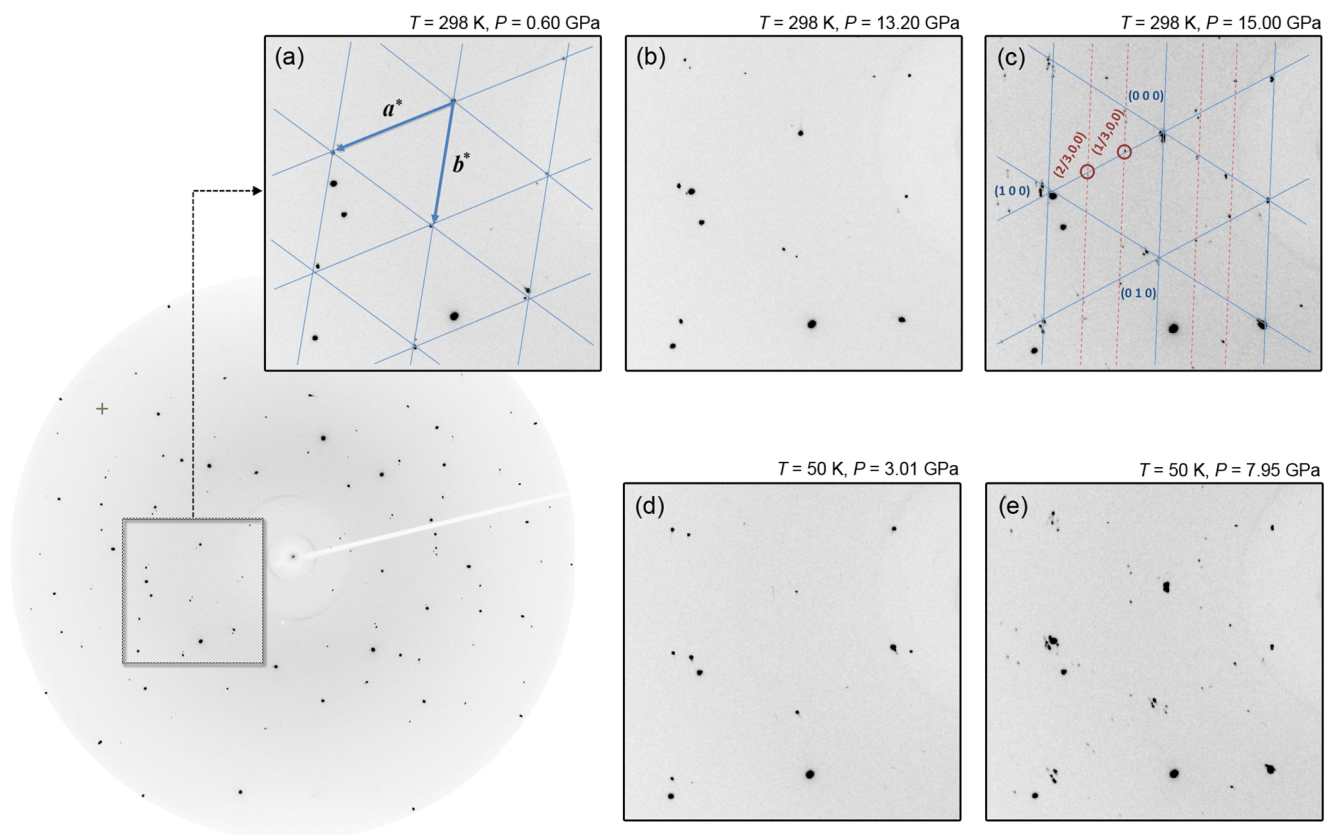


Figure 1. Diffraction images under different temperature–pressure conditions indicating a phase transition with superlattice reflections in $1T\text{-VSe}_2$. New peaks appear on the a -axis, as marked by dashed red lines, prior to the ambient lattice, which is denoted by the solid blue lines (unmarked images given in the Supporting Information). Here, a^* and b^* are the trigonal lattice parameters in the reciprocal space before the transition. Measurement data also revealed crystal twinning, which is evident by the presence of the additional symmetrical reflections. Note that this XRD measurement is not intended to show the CDW. Images may contain peaks from diamonds, Ne gas, and the cryostat window.

have contributed to enhancing our understanding of low-temperature physics of TMDs. However, phenomena related to the superstructure transitions under high pressure have yet to be explored comprehensively in these two-dimensional (2D) systems, although recent progress in this regard has been somewhat encouraging.^{6–10}

Vanadium diselenide (VSe_2), in its $1T$ polytype, has a superlattice incommensurate with the primitive lattice [i.e., a case of periodic lattice distortion coupled to charge density waves (PLD-CDW)], which is distinct from those in the other $1T$ or $2H$ TMDs because its CDW transition temperature increases with pressure.¹¹ The PLD-CDW superlattice in VSe_2 is characterized by a commensurate $4\mathbf{a}_0 \times 4\mathbf{a}_0$ superlattice forming in the layer plane and an incommensurate $\sim 3c_0$ superlattice forming perpendicularly to the layers at ~ 80 K.¹² The strong covalent bonding and small overlap of electron wave functions inside the metallic layers result in a quasi-two-dimensional character and a high anisotropy of the physical properties under ambient conditions. The layers are linked with weak van der Waals forces allowing various creative materials design possibilities, such as the intercalation of foreign atoms and molecules,¹³ exfoliation of the sample to the desired number of layers,^{14,15} and applications in electronic devices.^{16,17} Intriguingly, recent studies of VSe_2 revealed dramatic changes in the CDW and new physical properties such as a pseudogap, a Fermi arc, and emergent superconductivity;^{18–21} naturally, this motivates us to investigate the behavior of this material under high pressure.

In this study, by using the diamond-anvil cell (DAC),²² synchrotron X-ray diffraction (XRD), X-ray absorption (XAS), and first-principles calculations, we discovered an isostructural transition at ~ 6.5 GPa and a novel superstructure PLD phase at ~ 15 GPa occurring in $1T\text{-VSe}_2$. According to the XRD results and first-principles calculations, the high-pressure superstructure phase is associated with both the distortion of the structure and Fermi-surface nesting. The isostructural transitions in TMDs are commonly observed under high pressure.^{23,24} However, it is unusual that application of high pressure induces a new symmetrized phase with a superlattice, when pressure commonly suppresses such superstructures.

To investigate the superstructure and the phase transition at high pressure, we applied single-crystal zone-axis X-ray diffraction. This technique has been intensively used in transmission electron microscopy (TEM) and has recently also been introduced into the field of synchrotron single-crystal X-ray diffraction.^{25,26} The unique advantage of this technique lies in its ability to study very weak satellites in a tiny portion of the reciprocal space in the small-scattering angle region. We measured the diffraction patterns along the $[001]$ zone axis of $1T\text{-VSe}_2$ over a variable pressure–temperature range (with details given in the Supporting Information). During compression, a superlattice with commensurate peaks appeared along the original a -axis at ~ 15 GPa and 298 K (see Figure 1). Upon decreasing the temperature, we noticed that the transition temperature for the superlattice decreased with an increasing pressure within the experimental P – T range.

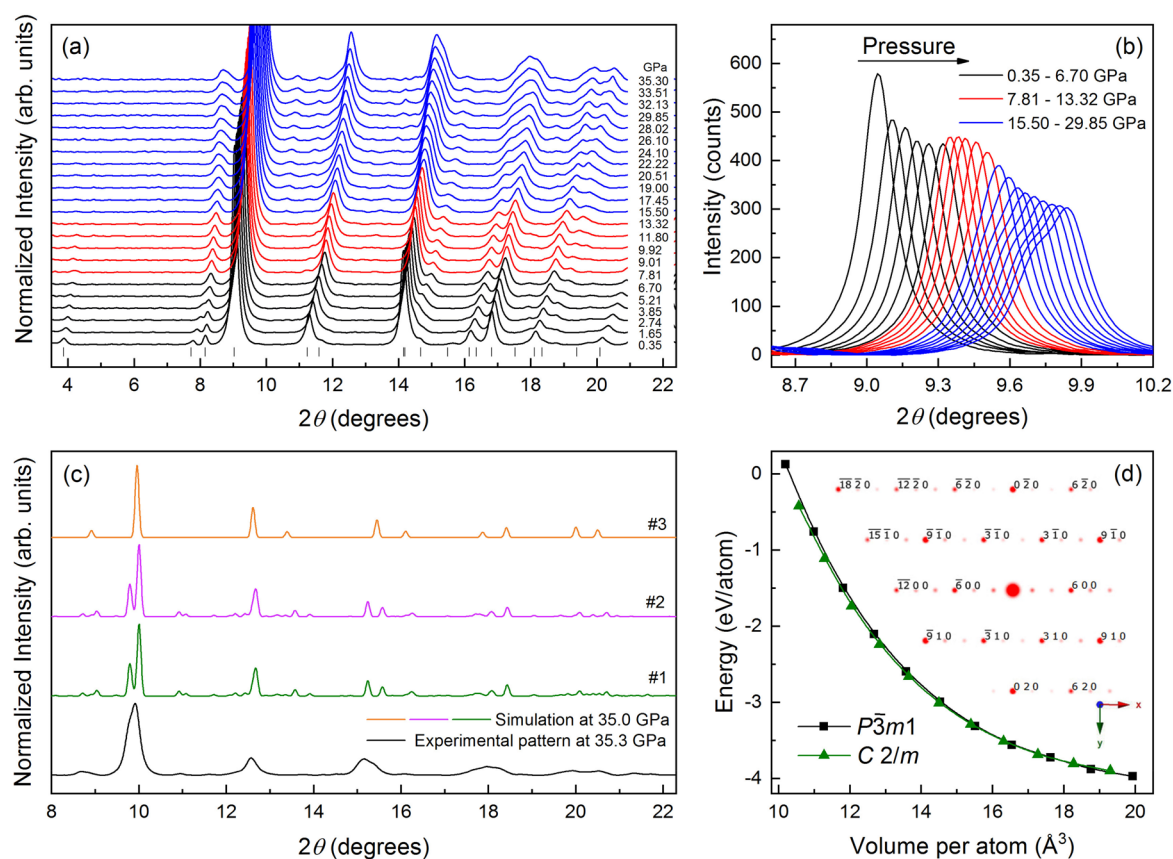


Figure 2. Synchrotron X-ray diffraction data for 1T-VSe₂ powders compared with the simulated results. The X-ray wavelength is 0.4133 Å. (a) Evolution of diffraction patterns over sample compression at room temperature. The positions of the initial $P\bar{3}m1$ Bragg reflections are marked by vertical bars. (b) Profile of the (011) peak at different ranges of pressure indicating its continuous intensity reduction and splitting. (c) Simulated XRD patterns for the high-pressure phase compared with experimental data at the same pressure. (d) Energies as a function of volume/atom calculated using GGA + U_{eff} . The inset shows a portion of the simulated reciprocal lattice of monoclinic phase 3 (full image given in the Supporting Information).

However, single-crystal zone-axis X-ray diffraction is limited by its small reception of the reciprocal space, incomplete peak profiles, and less accurate lattice parameters.^{25,26} Therefore, we also performed powder X-ray diffraction experiments to provide additional information about the larger reciprocal space in the large-scattering angle region, more accurate lattice parameters, and better peak profiles.

In Figure 2a, we show the phase transitions observed by synchrotron X-ray diffraction for 1T-VSe₂ powders. The structural transition occurs at 15.5 GPa, evidenced by a significant broadening of peak (011) and the appearance of new peaks in the diffraction patterns (Figure 2b). In the meantime, the single-crystal zone-axis diffraction also shows some satellites appearing at (1/3, 0, 0) at nearly the same pressure value, thereby suggesting a $3 \times 1 \times 1$ commensurate superstructure forming in a new symmetrized phase. By indexing the powder diffraction patterns of the new phase, we determined the sample transforms from trigonal $P\bar{3}m1$ into a monoclinic phase. Furthermore, powder X-ray diffraction measurements revealed an isostructural transition occurring around 6.7 GPa that is signaled by a sudden change in the pressure-dependent c/a ratio (see Figure 3b). A faster nonlinear decrease in the c/a ratio with pressure, before the transition, indicates that the cell parameter c is more compressible than a in this pressure range. Such anisotropic compressibility is attributed to the difference between the weaker van der Waals interlayer bonding and the stronger

intralayer covalent bonding. Then, a slower, roughly linear decrease in c/a , observed after the transition, suggests that the cell parameters a and c have nearly equal compressibility. The interlayer space hedged by Se atoms shrinks continuously under pressure, where the shortest distance between Se atoms decreases before finally resulting in bond formation at the structural transition (Figure 3d).

Determining a structure model directly from the powder X-ray diffraction patterns is challenging even under ambient conditions and becomes even more so in high-pressure environments where the background significantly complicates the intensity and profiles of the peaks. To tackle this problem, we created a $3 \times 3 \times 3$ supercell based on the structure at the ambient conditions and searched for a possible high-pressure structural model using evolutionary metadynamics²⁷ implemented in the USPEX software.²⁸ Then, the resultant structure models were optimized using the Vienna *ab initio* simulation package (VASP)²⁹ by minimizing the total energy and force on the atom with a converged criterion of $<10^{-4}$ eV/Å (with more details given in the Supporting Information). Three structure models were finally determined from the calculations, which all have superlattices with the same symmetry of $C2/m$ (No. 12) but in different unit cell shapes. (1) For model 1, $a = 11.7824$ Å, $b = 3.0502$ Å, $c = 12.0426$ Å, $\beta = 142.8996^\circ$, and $V = 261.07$ Å³. (2) For model 2, $a = 11.7824$ Å, $b = 3.0502$ Å, $c = 15.7368$ Å, $\beta = 152.5089^\circ$, and $V = 261.07$ Å³. (3) For model 3, $a = 15.9810$ Å, $b = 3.0744$ Å, $c = 5.3157$ Å, $\beta = 89.9929^\circ$, and $V =$

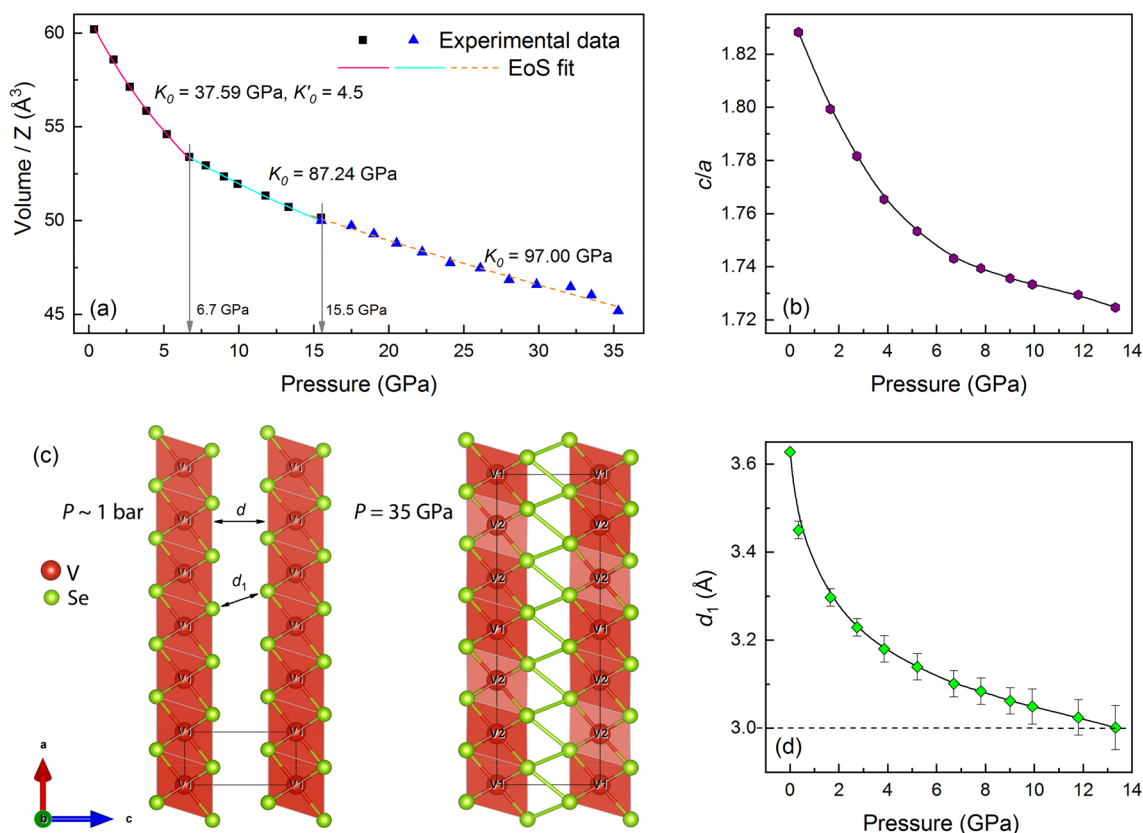


Figure 3. Changes of the unit cell in 1T-VSe₂ at different pressures. (a) Volumes per formula unit as a function of pressure for $P\bar{3}m1$ (black squares) and $C2/m$ (blue triangles) phases. The solid and dashed lines are the calculated third-order Birch–Murnaghan equation of state (EoS) fit to the experimental data. (b) Pressure dependence of the axial ratio c/a before the structural transition. (c) Crystal structure view of the a - c plane in the ambient $P\bar{3}m1$ phase and simulated high-pressure $C2/m$ phase (35 GPa pressure). Thick solid lines indicate the unit cell. 2D layers consist of vanadium-centered polyhedra stacked along the c -axis. (d) Pressure dependence of the shortest Se–Se distance d_1 in the interlayer space.

261.17 Å³. These three models have similar total energies for their ground states at high pressure. To benchmark the results from the prediction, we simulated the diffraction patterns to compare them with the experimental patterns (more details in the Supporting Information). The generated powder XRD patterns from the three models all match well with the experimental data (see Figure 2c), but only structure model 3 reproduces the experimental single-crystal zone-axis diffraction pattern (see the inset of Figure 2d and Figure S3); the other two models fail. In the zone-axis diffraction pattern of the high-pressure phase, the orientation of the $3 \times 1 \times 1$ supercell relative to the lattice of the original ambient phase is $a_{\text{super}} \parallel 3a_{\text{amb}}$; $b_{\text{super}} \parallel [110]_{\text{amb}}$; $c_{\text{super}} \parallel c_{\text{amb}}$.

The bulk modulus of the sample is obtained by fitting the pressure–volume data to the third-order Birch–Murnaghan equation of state (Figure 3a). For higher pressures, the increase in the bulk modulus with pressure indicates the hardening of the sample. The optimized structural model also reveals the origin of the $3 \times 1 \times 1$ high-pressure superstructure (Figure 3c). For instance, the high-pressure superstructure is quite similar to the structure of the ambient phase, which can be derived from the ambient-phase structure by displacing two V atoms (labeled as V2 in Figure 3c) out of the a - b plane with a small distance ($\sim 0.0026\%$ along the c -axis). Moreover, the octahedral site formed by one V2 atom and its surrounding six Se atoms is more distorted than other V-centered octahedral sites. It is the displacement of the V2 atom that breaks the original translation symmetry and results in a tripled

periodicity along the a -axis of the initial phase, as well as a new symmetrized structure. Such a superstructure manifests a structural distortion (in which V atoms deviate from their original positions and form a distorted octahedral site) that originates from the bonds forming between layers at high pressure.

In Figure 4, we plot the temperature–pressure-dependent structural change from trigonal $P\bar{3}m1$ to monoclinic $C2/m$ together with the CDW and superconductivity results from ref 21. Here, our data are consistent with CDW evolution, which is interrupted by the new structure at 12 GPa and 240 K. The fracture in the CDW onset curve at 4.5 GPa could be the same isostructural transition that we observed using powder XRD at 6.7 GPa (room temperature). The superconductivity appears after the CDW collapse in the superstructure at 15 GPa and 4 K.

To investigate how the transitions affect the electronic structures of the sample, we performed additional high-pressure XAS measurements at the Se K edge (~ 12.66 keV) to explore the unoccupied p bands of Se at high pressure. The room-temperature X-ray absorption near edge structure (XANES) (demonstrated in Figure 5) shows significant pressure dependency changes in a data region A (~ 12.67 keV). It is characterized by two trends T1 and T2, representing the peak energy position shift and the peak intensity decrease with broadening during sample compression, respectively. The pressure dependency changes in energy region A (Figure 5 and Figures S5–S7) are approximately standard for the unoccupied

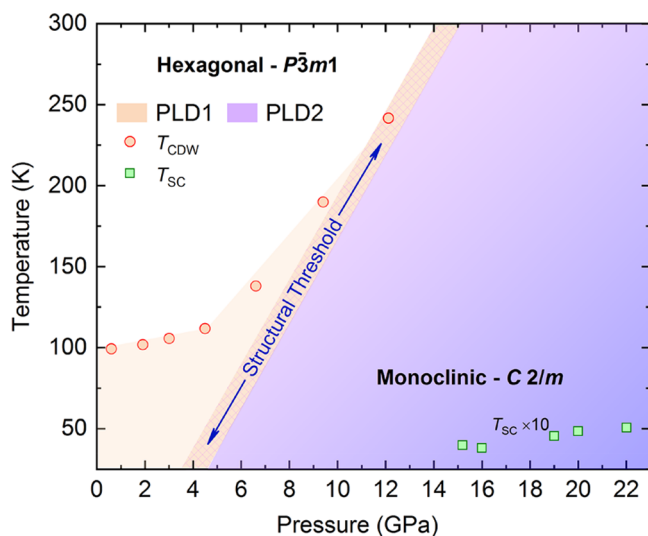


Figure 4. Structural changes in 1T-VSe₂ at different temperatures and pressures. Periodic lattice distortions in the pressure range from 0 to 23 GPa and a temperature range from 25 to 300 K for 1T-VSe₂. The structural threshold is drawn from our low-temperature single-crystal zone-axis XRD data. The data points for T_{CDW} and T_{SC} were taken from ref 21.

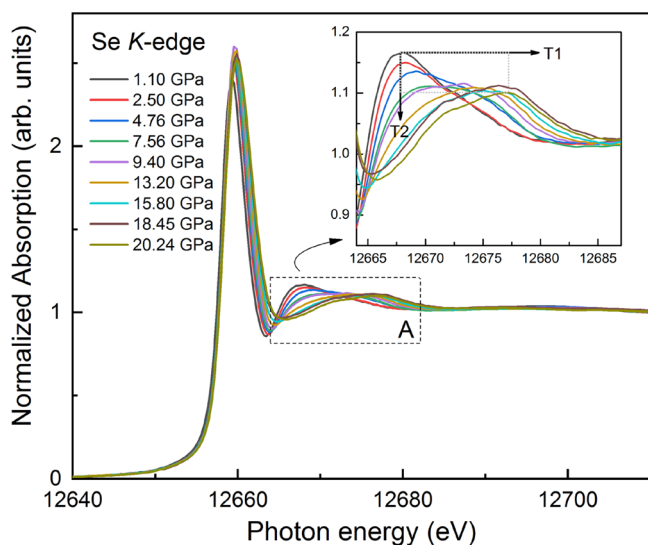


Figure 5. Normalized absorption spectra of 1T-VSe₂ at the Se K edge as a function of pressure. The inset shows zoomed area “A” where two trends T1 and T2 represent pressure-induced progressive feature peak position drifting and a feature peak intensity decrease, respectively.

DOS of Se p bands, which broaden significantly after the isostructural transition. The broadening of the occupied 4p bands is associated with bond formation (more delocalization) between the Se atoms in two different layers during the isostructural transition around 6.7 GPa. The isostructural transition eventually leads to the van der Waals force between layers evolving into the Heisenberg exchange interaction under pressure. In contrast, the transition at ~ 15.5 GPa causes no sizable changes in peak A, implying that the second transition has no dramatic effects on the Se p bands. This is consistent with the XRD result that the superstructure is mainly associated with the tiny displacement of V atoms. However, according to our first-principles calculations, it is noticeable that for the ambient phase in symmetry $P\bar{3}m1$, the density of

states (DOS) of vanadium at E_{F} is dominant, while for the high-pressure phase in symmetry $C2/m$, the DOS of selenium is increased substantially, “overwhelming” those of vanadium (Figure S8). The change in the orbital components at the Fermi level should be responsible for the continuous evolution of the XANES feature in energy region A observed in the XAS of the Se K edge. Intriguingly, the exfoliation of other TMDs does not change peak A in a similar fashion in X-ray absorption’s near edge structure.³⁰

Furthermore, in low-dimensional systems, the formation of a superlattice is usually associated with either structural distortion (e.g., electron–phonon coupling) or Fermi-surface nesting. Under ambient conditions, vanadium diselenide possesses a type II CDW with structural distortion (electron–phonon coupling).^{18,31} However, the high-pressure magneto-resistance and Hall measurements suggest successive electronic structural changes with Fermi-surface topology at 6 and 12 GPa, which match relatively well our defined isostructural and superlattice-type transitions, respectively. In addition, our calculations based on high-pressure structure model 3 (displayed in Figure 3c) also reveal a Fermi-surface nesting vector existing in the superstructure (Figure S9). Considering that the structural distortion and the Fermi-surface nesting vector both exist in the new superstructure phase, the origin of the superstructure may be a Fermi-surface nesting-driven periodic lattice distortion.

In conclusion, our experimental XRD and XAS room-temperature high-pressure studies revealed that 1T-VSe₂ undergoes two transitions: an isostructural one at 6.7 GPa and a structural one at 15.5 GPa. The first transition was associated with layer sliding and anisotropic–isotropic–contraction change between lattice parameters. At this transition, the weak van der Waals bonds between layers eventually transform into the strong covalent bonds under pressure. The second transition induces a $3 \times 1 \times 1$ superstructure, which has a symmetry lower than $P\bar{3}m1$. Using theoretical structure-prediction tools, we found that the new phase should be monoclinic $C2/m$ where the superstructure is associated with the displacement of V atoms. The first-principles calculations suggest that Fermi-surface nesting is involved in superlattice formation because the high-pressure phase contains wave vectors of the electrons corresponding to the Fermi energy. This exciting (and, to the best of our knowledge, unique) discovery proves that superstructure not only emerges in two-dimensional structures but paves the way for pressure tuning of three-dimensional structures for manipulating and engineering novel symmetry for disparate real-world applications, such as developing superconductivity.

■ ASSOCIATED CONTENT

Supporting Information

The Supporting Information is available free of charge at <https://pubs.acs.org/doi/10.1021/acs.jpcllett.9b03247>.

Detailed calculations, further numerical results, and further analysis of experimental data (PDF)

■ AUTHOR INFORMATION

Corresponding Authors

*E-mail: raimundas.sereika@hpstar.ac.cn.

*E-mail: yang.ding@hpstar.ac.cn.

ORCID

Raimundas Sereika: 0000-0001-5365-6773

Changyong Park: 0000-0002-3363-5788

Niall J. English: 0000-0002-8460-3540

Hechang Lei: 0000-0003-0850-8514

Steve M. Heald: 0000-0002-4369-8248

Notes

The authors declare no competing financial interest.

ACKNOWLEDGMENTS

Portions of this work were performed at HPCAT (Sector 16) and XSD (Sector 20) of the Advanced Photon Source (APS), Argonne National Laboratory. HPCAT operations are supported by DOE-NSNSA's Office of Experimental Sciences. XSD operations are supported by the U.S. Department of Energy (DOE) and the Canadian Light Source (CLS). The APS is a DOE Office of Science User Facility operated for the DOE Office of Science by Argonne National Laboratory under Contract DE-AC02-06CH11357. Y.D. acknowledges support from the National Key Research and Development Program of China No. 2018YFA0305703, NSAF grant No. U1930401, NSFC No. 11874075, and Challenge project No. TZ2016001. We also acknowledge financial support from the NSFC under grant numbers U1530402 and 11811530001. H.L. acknowledges support from the National Key Research and Development Program of China (2016YFA0300504), the NSFC (11574394, 11774423, and 11822412), the Fundamental Research Funds for the Central Universities, and the Research Funds of Renmin University of China (RUC) (15XNLQ07, 18XNLG14, and 19XNLG17). S.B. and N.J.E. thank Science Foundation Ireland for support under the SFI-NSFC bilateral programme (SFI 17/NSFC/5229).

REFERENCES

- (1) Sipos, B.; Kusmartseva, A. F.; Akrap, A.; Berger, H.; Forró, L.; Tutiš, E. From Mott state to superconductivity in 1T-TaS₂. *Nat. Mater.* **2008**, *7*, 960–965.
- (2) Kusmartseva, A. F.; Sipos, B.; Berger, H.; Forró, L.; Tutiš, E. Pressure Induced Superconductivity in Pristine 1T-TiSe₂. *Phys. Rev. Lett.* **2009**, *103*, 236401.
- (3) Nayak, A. P.; Bhattacharyya, S.; Zhu, J.; Liu, J.; Wu, X.; Pandey, T.; Jin, C.; Singh, A. K.; Akinwande, D.; Lin, J.-F. Pressure-induced semiconducting to metallic transition in multilayered molybdenum disulphide. *Nat. Commun.* **2014**, *5*, 3731.
- (4) Rossmagel, K. On the origin of charge-density waves in select layered transition-metal dichalcogenides. *J. Phys.: Condens. Matter* **2011**, *23*, 213001.
- (5) Weber, F.; Rosenkranz, S.; Castellán, J.-P.; Osborn, R.; Hott, R.; Heid, R.; Bohnen, K.-P.; Egami, T.; Said, A. H.; Reznik, D. Extended Phonon Collapse and the Origin of the Charge-Density Wave in 2H-NbSe₂. *Phys. Rev. Lett.* **2011**, *107*, 107403.
- (6) Zhao, Z.; Zhang, H.; Yuan, H.; Wang, S.; Lin, Y.; Zeng, Q.; Xu, G.; Liu, Z.; Solanki, G. K.; Patel, K. D.; Cui, Y.; Hwang, H. Y.; Mao, W. L. Pressure induced metallization with absence of structural transition in layered molybdenum diselenide. *Nat. Commun.* **2015**, *6*, 7312.
- (7) Ma, Y.; Dai, Y.; Guo, M.; Niu, C.; Zhu, Y.; Huang, B. Evidence of the Existence of Magnetism in Pristine VX₂Monolayers (X = S, Se) and Their Strain-Induced Tunable Magnetic Properties. *ACS Nano* **2012**, *6*, 1695–1701.
- (8) Ying, J.; Paudyal, H.; Heil, C.; Chen, X.-J.; Struzhkin, V. V.; Margine, E. R. Unusual Pressure-Induced Periodic Lattice Distortion in SnSe₂. *Phys. Rev. Lett.* **2018**, *121*, 027003.
- (9) Wang, B.; Liu, Y.; Ishigaki, K.; Matsubayashi, K.; Cheng, J.; Lu, W.; Sun, Y.; Uwatoko, Y. Pressure-induced bulk superconductivity in a layered transition-metal dichalcogenide 1T-tantalum selenium. *Phys. Rev. B: Condens. Matter Mater. Phys.* **2017**, *95*, No. 220501(R).

(10) Dutta, U.; Malavi, P. S.; Sahoo, S.; Joseph, B.; Karmakar, S. Pressure-induced superconductivity in semimetallic 1T-TiTe₂ and its persistence upon decompression. *Phys. Rev. B: Condens. Matter Mater. Phys.* **2018**, *97*, No. 060503(R).

(11) Friend, R. H.; Jerome, D.; Schleich, D. M.; Molinie, P. Pressure Enhancement of Charge Density Wave Formation in VSe₂; The Role of Coulomb Correlations. *Solid State Commun.* **1978**, *27*, 169–173. Original paper: Chan, S.-K.; Heine, V. Spin density wave and soft phonon mode from nesting Fermi surfaces. *J. Phys. F: Met. Phys.* **1973**, *3*, 795.

(12) Giambattista, B.; Slough, C. G.; McNairy, W. W.; Coleman, R. V. Scanning tunneling microscopy of atoms and charge-density waves in 1T-TaS₂, 1T-TaSe₂, and 1T-VSe₂. *Phys. Rev. B: Condens. Matter Mater. Phys.* **1990**, *41*, 10082.

(13) Ekvall, I.; Brauer, H. E.; Wahlström, E.; Olin, H. Locally modified charge-density waves in Na intercalated VSe₂ studied by scanning tunneling microscopy and spectroscopy. *Phys. Rev. B: Condens. Matter Mater. Phys.* **1999**, *59*, 7751.

(14) Wang, Y.; Sofer, Z.; Luxa, J.; Pumera, M. Lithium Exfoliated Vanadium Dichalcogenides (VS₂, VSe₂, VTe₂) Exhibit Dramatically Different Properties from Their Bulk Counterparts. *Adv. Mater. Interfaces* **2016**, *3*, 1600433.

(15) Pásztor, A.; Scarfato, A.; Barreateau, C.; Giannini, E.; Renner, C. Dimensional crossover of the charge density wave transition in thin exfoliated VSe₂. *2D Mater.* **2017**, *4*, 041005.

(16) Zhang, Z.; Niu, J.; Yang, P.; Gong, Y.; Ji, Q.; Shi, J.; Fang, Q.; Jiang, S.; Li, H.; Zhou, X.; Gu, L.; Wu, X.; Zhang, Y. Van der Waals Epitaxial Growth of 2D Metallic Vanadium Diselenide Single Crystals and their Extra-High Electrical Conductivity. *Adv. Mater.* **2017**, *29*, 1702359.

(17) Wang, C.; Wu, X.; Ma, Y.; Mu, G.; Li, Y.; Luo, C.; Xu, H.; Zhang, Y.; Yang, J.; Tang, X.; Zhang, J.; Bao, W.; Duan, C. Metallic few-layered VSe₂ nanosheets: high twodimensional conductivity for flexible in-plane solidstate supercapacitors. *J. Mater. Chem. A* **2018**, *6*, 8299–8306.

(18) Chen, P.; Pai, W. W.; Chan, Y.-H.; Madhavan, V.; Chou, M. Y.; Mo, S.-K.; Fedorov, A.-V.; Chiang, T.-C. Unique Gap Structure and Symmetry of the Charge Density Wave in Single-Layer VSe₂. *Phys. Rev. Lett.* **2018**, *121*, 196402.

(19) Feng, J.; Biswas, D.; Rajan, A.; Watson, M. D.; Mazzola, F.; Clark, O. J.; Underwood, K.; Markovic, I.; McLaren, M.; Hunter, A.; Burn, D. M.; Duffy, L.; Barua, S.; Balakrishnan, G.; Bertran, F.; Le Fevre, P.; Kim, T.; van der Laan, G.; Hesjedal, T.; Wahl, P.; King, P. D. C. Electronic Structure and Enhanced Charge-Density Wave Order of Monolayer VSe₂. *Nano Lett.* **2018**, *18*, 4493–4499.

(20) Umamoto, Y.; Sugawara, K.; Nakata, Y.; Takahashi, T.; Sato, T. Pseudogap, Fermi arc, and Peierls-insulating phase induced by 3D–2D crossover in monolayer VSe₂. *Nano Res.* **2019**, *12*, 165–169.

(21) Sahoo, S.; Dutta, U.; Harnagea, L.; Sood, A. K.; Karmakar, S. Pressure-induced suppression of charge density wave and emergence of Superconductivity in 1T-VSe₂. *arXiv* **2019**, 1908.11678.

(22) Mao, H.-K.; Chen, X.; Ding, Y.; Li, B.; Wang, L. Solids, liquids, and gases under high pressure. *Rev. Mod. Phys.* **2018**, *90*, 015007.

(23) Wang, X.; Chen, X.; Zhou, Y.; Park, C.; An, C.; Zhou, Y.; Zhang, R.; Gu, C.; Yang, W.; Yang, Z. Pressure-induced iso-structural phase transition and metallization in WSe₂. *Sci. Rep.* **2017**, *7*, 46694.

(24) Rajaji, V.; Dutta, U.; Sreeparvathy, P. C.; Sarma, S. C.; Sorb, Y. A.; Joseph, B.; Sahoo, S.; Peter, S. C.; Kanchana, V.; Narayana, C. Structural, vibrational, and electrical properties of 1T-TiTe₂ under hydrostatic pressure: Experiments and theory. *Phys. Rev. B: Condens. Matter Mater. Phys.* **2018**, *97*, 085107.

(25) Ding, Y.; Liu, H.; Xu, J.; Prewitt, C. T.; Hemley, R. J.; Mao, H.-K. Zone-axis diffraction study of pressure-induced inhomogeneity in single-crystal Fe_{1-x}O. *Appl. Phys. Lett.* **2005**, *87*, 041912.

(26) Ding, Y.; Liu, H.; Somayazulu, M.; Meng, Y.; Xu, J.; Prewitt, C. T.; Hemley, R. J.; Mao, H.-K. Zone-axis x-ray diffraction of single-crystal Fe_{1-x}O under pressure. *Phys. Rev. B: Condens. Matter Mater. Phys.* **2005**, *72*, 174109.

(27) Zhu, Q.; Oganov, A. R.; Lyakhov, A. O. Evolutionary metadynamics: a novel method to predict crystal structures. *CrystEngComm* **2012**, *14*, 3596.

(28) Lyakhov, A. O.; Oganov, A. R.; Stokes, H. T.; Zhu, Q. New developments in evolutionary structure prediction algorithm USPEX. *Comput. Phys. Commun.* **2013**, *184*, 1172–1182.

(29) Kresse, G.; Furthmüller, J. Efficient iterative schemes for *ab initio* total-energy calculations using a plane-wave basis set. *Phys. Rev. B: Condens. Matter Mater. Phys.* **1996**, *54*, 11169–11186.

(30) Gordon, R. A.; Yang, D.; Crozier, E. D.; Jiang, D. T.; Frindt, R. F. Structures of exfoliated single layers of WS₂, MoS₂, and MoSe₂ in aqueous suspension. *Phys. Rev. B: Condens. Matter Mater. Phys.* **2002**, *65*, 125407.

(31) Zhu, X.; Cao, Y.; Zhang, J.; Plummer, E. W.; Guo, J. Classification of charge density waves based on their nature. *Proc. Natl. Acad. Sci. U. S. A.* **2015**, *112*, 2367–2371.